Liu *et al. Cell Division* (2024) 19:32
https://doi.org/10.1186/s13008-024-00136-8

Cell Division

RESEARCH Open Access

The E3 ubiquitin ligase RNF6 facilitates the progression of cervical cancer by inhibiting the Hippo/Yap pathway

Yawen Liu[1†], Juanjuan Zhou[2,3†], Weiqi Liu[2,3†], Yi Le[2,3], Lingling Zhang[1], Ziyu Zhang[1], Ling Zhou[2,3*] and Ling Li[1*]

Abstract

Purpose Cervical cancer (CC), a significant global health threat, necessitates comprehensive understanding for improved therapeutic interventions. Many research indicates that dysregulation of the Hippo-YAP1 pathway leads to uncontrolled proliferation and invasion of tumor cells, promoting the progression of various cancers. This article aims to elucidate the role of RNF6 in CC and its regulation of the Hippo-YAP1 signaling pathway.

Methods The public tumor dataset analyses, immunohistochemistry, and western blotting were used to explore the expression of RNF6 in CC. Gain- and loss-of-function assays were conducted to elucidate the role of RNF6 in the proliferation and invasion of CC cells. Transcriptome sequencing was used to explore RNF6's role in cervical cancer, with validation of its regulation of the Hippo-YAP1 pathway through western blotting and RT-qPCR. Co-transfection of YAP overexpression plasmids into RNF6-silenced CC cells were preformed to confirm YAP1's pivotal role in RNF6-mediated CC progression. Animal experiments were preformed to further validate RNF6 interference's inhibitory effect on CC proliferation in vivo.

Results Clinical samples and bioinformatics analysis revealed high expression of RNF6 in CC, and closely associated with advanced FIGO (International Federation of Gynecology and Obstetrics) stage, larger tumor size, and poor prognosis. Cellular functional experiments demonstrate that RNF6 promotes the proliferation, invasion, and migration of CC cells, while knockdown of RNF6 yields the opposite effect. Transcriptome sequencing further reveals that RNF6 may promote CC progression through the Hippo-YAP signaling pathway. Western blotting and RT-qPCR further unveil that RNF6 enhances the upregulation of YAP1 protein levels, thereby activating downstream oncogenes CTGF and CYR61 transcription. Additionally, exogenous overexpression of YAP1 reverses the inhibitory effect of RNF6 silencing on CC proliferation and invasion. Furthermore, RNF6 interference significantly attenuates tumor growth in vivo experiments.

†Yawen Liu, Juanjuan Zhou and Weiqi Liu contributed equally to this work.

*Correspondence:
Ling Zhou
363006210002@email.ncu.edu.cn
Ling Li
liling_hot1@163.com

Full list of author information is available at the end of the article

Conclusion Our research reveals that RNF6 is highly expressed in CC, driving malignant progression by upregulating YAP1 protein expression and enhancing the transcription of downstream target genes CTGF and CYR61, offering potential therapeutic targets for CC treatment.

Keywords Cervical cancer, RNF6, YAP1, Proliferation, Invasion and migration

Introduction

Cervical cancer (CC) stands as a significant gynecological cancer worldwide, presenting a considerable risk to women's health [1]. A disproportionate (70%) of these cases occur in less developed regions [2]. The widespread adoption of cervical cytology screening and HPV vaccination has significantly increased the early detection rate and prevention efficacy of cervical cancer [3–5]. Modern medical treatments for CC typically include surgery, radiotherapy, chemotherapy, and others. Despite advancements in CC treatment, late-stage CC patients face lower survival rates due to tumor recurrence and metastasis [6]. The exact molecular mechanisms leading to the development of cervical tumors remain to be fully unraveled, making it imperative to explore these mechanisms further.

The Hippo signaling pathway, a key regulator in cell growth and organ size, has been identified as playing a pivotal role in cancer cell invasion and migration [7]. This pathway involves a cascade of kinases, including MST1/2 and LATS1/2, and the transcriptional coactivators YAP/TAZ [8, 9]. Upon stimulation by upstream kinases, MST1/2 phosphorylate LATS1/2. Subsequently, phosphorylated LATS1/2 further phosphorylate YAP1, leading to its degradation and inactivation in the cytoplasm. Conversely, unphosphorylated YAP1 moves into the cell nucleus and binds to transcription factors such as TEAD, activating downstream targets like CTGF and CYR61, and further promotes tumorigenesis [10, 11]. Therefore, the protein level and subcellular localization of YAP1 are crucial. Recent advances have supported the role of YAP dysregulation in tumorigenesis, particularly in gynecological tumors [12]. However, further clarification is needed regarding YAP's role in cervical cancer and the associated regulatory mechanisms.

Ring finger protein 6 (RNF6), an E3 ubiquitin ligase, facilitates the degradation of its target proteins through the ubiquitin-proteasome pathway, playing a crucial role in cancer cell growth and survival [13, 14]. Mounting evidence indicates that RNF6 plays a role in the progression of diverse cancers, such as gastric cancer, esophageal squamous cell carcinoma, lung adenocarcinoma, breast cancer, and numerous others [13, 15–17]. RNF6 targets the key molecules to activate or inhibit signaling pathways, and further controls the malignant physiological characteristics of tumors. For instance, RNF6 enhances the advancement of colorectal cancer by activating the Wnt/β-catenin pathway through ubiquitination of TLE3, or by suppressing GSK-3β [18, 19]. And it promotes EMT in esophageal squamous cell carcinoma by activating the TGF-β1/c-Myc pathway [20]. However, the impact of RNF6 on CC and its underlying mechanisms remain unclear.

In this study, we found that RNF6 plays a crucial role in the occurrence and progression of CC partially through the modulation of the Hippo-YAP signaling pathway. Upregulation of RNF6 promotes CC cell growth, migration, and invasion, while reducing RNF6 levels was observed to have the opposite effect. Mechanistically, RNF6 upregulates the protein level of YAP1, thereby activating the transcription of oncogenes such as CTGF and CYR61. In summary, our study underscores the pivotal role of the RNF6-mediated Hippo-YAP1 pathway in driving the advancement of CC. These findings offer fresh perspectives on therapeutic targets that could benefit individuals with CC.

Results

RNF6 was high expressed in CC and correlated with poor prognosis in patients

To investigate the role of RNF6 in tumors, we initially employed the TIMER database (http://timer.cistrome.org/) to analyze the expression of RNF6 in various tumor tissues and corresponding adjacent tissues. The analysis revealed significant expression differences of RNF6 in multiple tumors (Fig. 1A), suggesting its potential significance in the initiation and progression of cancer. In CC, RNF6 expression was found to be higher in tumor tissues compared to normal cervical tissues. However, due to the limited number of normal samples (only three cases), we utilized the GEPIA database (http://gepia.cancer-pku.cn/) to analyze 306 CC tissues and 13 normal cervical tissues from GTEx and TCGA. The results confirmed the elevated expression of RNF6 in CC tissues (Fig. 1B). Additionally, we performed survival analysis on CC patients from TCGA and the findings indicated that patients with high RNF6 expression had significantly shorter overall survival (OS) and disease-free survival (DFS) compared to those with low expression (Fig. 1C, D). Results from the Kaplan-Meier plotter website (https://kmplot.com/analysis/) further emphasized the superior overall survival (OS) and recurrence-free survival (RFS) in CC patients with lower RNF6 expression (Fig. 1E, F). Furthermore, we conducted IHC staining on tumor tissues and adjacent tissues from 149 CC patients in our hospital, followed by scoring and statistical analysis. The

results also demonstrated higher expression levels of RNF6 in tumor tissues (Fig. 1H), correlating with adverse pathological features such as FIGO stage and tumor size (Fig. 1G; Table 1). CC patients with high RNF6 expression exhibited poorer OS and progression-free survival (PFS) compared to those with low expression (Fig. 1I, J). Collectively, these findings suggest that RNF6 was higher expressed in CC and correlated with poor prognosis in patients.

Regulation of RNF6 expression influences the malignant behavior of CC cells in vitro

To elucidate the role of RNF6 in CC cells, we overexpressed and downregulated RNF6 in SiHa and HeLa cells, respectively, and observed alterations in the malignant biological behavior of the cells. We first verified the transfection efficiency of RNF6 expression constructs by western blotting (Figs. 2A and 3A). Through CCK-8 and colony formation assays, we observed that ectopic expression of RNF6 enhanced the growth and colony-forming ability of SiHa and HeLa cells (Fig. 2B, C). Depletion of RNF6 exhibited opposite effects (Fig. 3B-D). Moreover, RNF6 overexpression augmented the migration and invasion capabilities of CC cells (Fig. 2D, E), while silencing RNF6 produced opposite effects (Fig. 3E-H). In summary, these data indicate that RNF6 expression was associated with the proliferation, migration, and invasion of CC cells in vitro, suggesting its potential as a therapeutic target for CC patients.

RNF6 exerts regulatory effects on the YAP signaling pathway

In order to understand how RNF6 plays a role in promoting the proliferation and invasion of CC cells, we transfected HeLa cells with RNF6 overexpression plasmid and performed transcriptome sequencing. Through sequencing, we identified 137 genes upregulated and 131 genes downregulated in the RNF6 overexpression group compared to the control group. We presented a heat map illustrating some differentially expressed genes and a volcano plot depicting the overall expression profile of all genes, highlighting the differentially expressed genes (Fig. 4A, B). The above differentially expressed genes were subjected to KEGG pathway enrichment analysis, the results revealing that RNF6 may regulate the Hippo-YAP signaling pathway (Fig. 4C). We employed western blotting and RT-qPCR experiments to validate the sequencing conclusions. The results indicated that YAP1 protein, as well as the protein and mRNA levels of downstream target genes CYR61 and CTGF, were downregulated following the depletion of RNF6 in HeLa and SiHa cells. Conversely, ectopic expression of RNF6 resulted in the upregulation of YAP1, CYR61 and CTGF (Fig. 4D and E). The above data collectively suggest that RNF6 activates the Hippo-YAP signaling pathway.

Ectopic expression of YAP1 reverses the functional phenotypes induced by RNF6 deficiency in CC

To further investigate whether the YAP pathway was indispensable in RNF6-mediated CC progression, we use siRNA and plasmids to manipulate the expression of RNF6 and YAP1 in HeLa cells, assessing malignant characteristics and protein alterations. As shown in Fig. 5A, RNF6 siRNA reduced the expression of the core component of the Hippo signaling pathway, YAP1. However, ectopic expression of YAP1 nullified the inhibitory effect of RNF6 knockdown (Fig. 5A). Functional analyses further confirmed that the suppression of proliferation, migration, and invasion induced by RNF6 silencing in CC cells was largely rescued by overexpression of YAP1 (Fig. 5B-G). In conclusion, these data suggest a crucial role of the YAP1 in mediating the promotion of human CC cell progression by RNF6.

The depletion of RNF6 attenuated the proliferation of CC cells in vivo

To elucidate the impact of RNF6 on tumorigenesis of CC cells more credible, we established a xenograft model by inoculating subcutaneously RNF6-knockdown HeLa cells into the right armpit of BALB/c nude mice, and closely monitoring tumor size for 28 days. Compared to the controls, the tumor growth and weight in the RNF6-knockdown group were significantly reduced (Fig. 6A, B, D, $P<0.05$). Consistent with previous results in vitro experiments, western blotting analysis of xenograft tissues showed that YAP1 protein was markedly decreased in RNF6-knockdown group (Fig. 6C). In conclusion, these results suggest that RNF6 depletion inhibits tumor growth in vivo by modulating the YAP1 pathway.

Discussion

Our study delves into the intricate molecular mechanisms underlying CC, highlighting the pivotal role of RNF6 in the malignant progression of this disease. Our findings demonstrate a significant upregulation of RNF6 in CC tumor tissues, correlating with a more aggressive phenotype. Cellular functional experiments confirmed that RNF6 promoted the proliferation, invasion and migration of CC cells. Unraveling mechanistic details, we found that RNF6 overexpression increases YAP1 protein levels, leading to the activation of CTFG and CYR61 transcription.

The Hippo-YAP signaling pathway plays a crucial role in regulating organ size and cell proliferation, and its aberrant regulation is essential in the initiation and progression of carcinogenesis [21]. Elevated YAP1 protein levels, a core component of the Hippo pathway, have

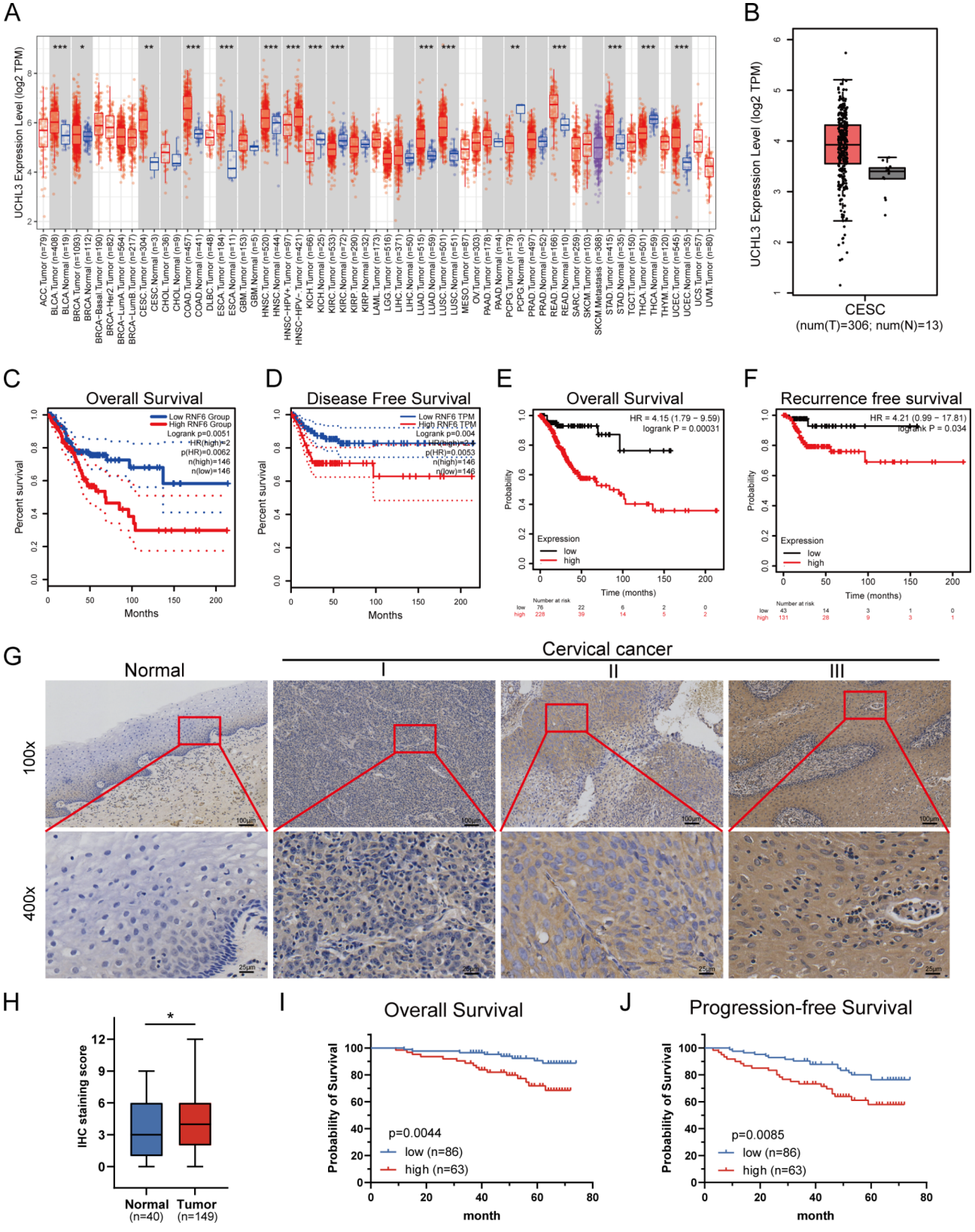

Fig. 1 (See legend on next page.)

(See figure on previous page.)

Fig. 1 RNF6 was high expressed in CC and correlated with poor prognosis in patients. (**A**) Comparisons of RNF6 expression levels between various tumor tissues and their corresponding normal tissues using TCGA data from the TIMER database. (**B**) RNF6 mRNA expression in cervical cancer (CC) tissues compared with normal cervical epithelial tissue according to the GEPIA database. (**C**, **D**) Prognostic associations, encompassing overall survival (OS) and disease-free survival (DFS), among CC patients using GEPIA database. (**E**, **F**) Prognostic associations, including OS and recurrence-free survival (RFS), in CC patients according to the KM-Plotter database. (**G**) Representative immunohistochemistry (IHC) staining images showing RNF6 protein expression in human CC tissues compared to adjacent cervical epithelial tissue. (**H**) Statistical results of IHC scoring presented with a box plot. (**I**, **J**) Comparison of patients with higher RNF6 expression levels ($n=63$) to those with lower RNF6 expression ($n=86$) using Kaplan-Meier survival analysis, comprising OS and progression-free survival (PFS). $^{*}p<0.05$; $^{**}p<0.01$

been implicated in various human cancers, including cervical, breast, bladder, and colon cancers [22–25]. Preclinical data strongly advocate for the therapeutic targeting of YAP1-TEADs, suggesting its potential as a promising strategy in cancer treatment [26]. The introduction of the first clinical data on VT3989, a drug targeting the Hippo-YAP pathway, at the 2023 AACR annual meeting further underscores the clinical relevance of our findings [27]. This clinical data presents VT3989 as a potential therapeutic avenue for solid tumors, emphasizing the prospect of targeting YAP1-TEADs in the treatment of this malignancy. Intriguingly, we found for the first time that RNF6 is an upstream regulator of YAP1 protein in CC. RNF6 is frequently upregulated in human cancers such as colorectal, gastric, and liver cancers [28–30]. For example, RNF6 is overexpressed in hepatocellular carcinoma and promotes tumor metastasis and radiotherapy resistance.by binding and ubiquitinating forkhead box protein A1 (FoxA1), an important transcriptional suppressor of the EMT process [14]. In this study, we demonstrated for the first time that high expression of RNF6 is strongly associated with poor prognosis in 149 real-world CC samples. Our research resonates with the work of Kang Zhu and his colleagues in understanding RNF6's involvement in cancer biology [31]. Compared to their observations in HeLa cells, our functional experiments, encompassing gain-of-function and loss-of-function assays, emphasize RNF6's role in promoting the proliferative capacity of CC cells. Furthermore, our study expands on their work by elucidating RNF6's influence on migration and invasion capabilities in CC cells. Distinctively, our research reveals RNF6 as an upstream regulator of YAP1, providing a more nuanced understanding of its impact on the biological behavior of CC cells.

RNF6, situated on chromosome 13q12.13 [32], has been recognized as a member of the RNF family, known for mediating ubiquitination and orchestrating the degradation of its target proteins within proteasomes [19]. Existing studies have unveiled the involvement of various RNF family members in the intricate regulation of cellular proliferation and differentiation, functioning either as oncogenes or tumor suppressors depending on their specific target proteins and cellular context [33]. A meticulous literature review revealed that RNF6 plays a pivotal role in cancer promotion through ubiquitination and transcriptional regulation [34]. In terms of ubiquitination, RNF6 activates the Wnt/β-Catenin pathway in colorectal cancer by ubiquitinating TLE3 [19]. It further facilitates breast cancer migration and invasion by promoting the ubiquitination and degradation of MST1 [13]. Additionally, RNF6 promotes metastasis and radioresistance in hepatocellular carcinoma through the ubiquitination of FoxA1 [14]. On the transcriptional regulation front, RNF6 contributes to colorectal tumorigenesis by transcriptionally activating SF3B2 [35], and it enhances gastric cancer progression through the regulation of CCNA1/CREBBP transcription [15]. Our study provides novel insights into the role of RNF6 in CC, demonstrating that an increase in RNF6 levels correlates with elevated YAP1 protein without a corresponding impact on YAP1 mRNA levels. This observation leads us to speculate that RNF6 exerts its influence on YAP1 specifically at the protein level through ubiquitination. However, further investigations are warranted to elucidate whether YAP1 is a direct target of RNF6 and the specific modifications involved in this process. The findings by others, demonstrating that RNF6 modulates the Hippo/YAP signaling pathway by ubiquitinating and degrading MST1, thereby promoting breast cancer progression [13], significantly contribute to the relevance of our study. These results underscore the regulatory network of RNF6 and its critical role in cancer, providing valuable insights that enhance our understanding of its potential therapeutic implications.

Materials and methods

Tissue samples and ethical considerations

We acquired 150 paraffin-embedded specimens from CC patients who underwent surgery at Jiangxi Provincial Maternal and Child Health Hospital between 2017 and 2018, with no prior history of anti-tumor therapy. Table 1 outlines the clinicopathological features of the CC patients. The study received ethical approval from the relevant committee and followed the principles of the Declaration of Helsinki. All participating patients provided written informed consent.

Cell culturing and genetic modification techniques

The human CC lines, HeLa and SiHa, were procured from the China Academy of Sciences' Shanghai Institute of Cell Biology. These CC cells were maintained in a controlled environment using Dulbecco's Modified Eagle

Table 1 Association of UCHL3 RNF6 levels with clinical and pathological features of cervical cancer patients

Characteristics	*N*	RNF6 expression		*P*-value
		Low	High	
Age, years				
≤ 45	53	31 (20.8%)	22 (14.8%)	0.887
> 45	96	55 (36.9%)	41 (27.5%)	
Histological type				
Squamous cell carcinoma	127	72 (48.3%)	55 (36.9%)	0.863
Adenocarcinoma	17	11 (7.4%)	6 (4.0%)	
Adenosquamous carcinoma	5	3(2.0%)	2(1.3%)	
Tumor size, cm				
≤ 3	51	37 (24.8%)	14 (9.4%)	**0.008**
> 3	98	49 (32.9%)	49 (32.9%)	
FIGO stage				
I-II	114	73(49.0%)	41 (27.5%)	**0.005**
III-IV	35	13 (8.7%)	22 (14.8%)	
Lymph node metastasis				
No	63	37 (24.8%)	26 (17.5%)	0.831
Yes	86	49 (32.9%)	37 (24.8%)	

P-values determined using χ2 test

Medium (DMEM, HyClone, Logan, UT, USA), enriched with 10% fetal bovine serum (FBS; BI, Kibbutz, Israel), within a 5% CO_2 atmosphere at 37 °C. The authenticity of each cell line was confirmed by short tandem repeat (STR) analysis, with routine mycoplasma testing every three months.

Transfection procedures were executed utilizing the TurboFect reagent (Thermo Scientific, R0532, Waltham, USA), with siRNA sourced from Gempharmatech (Jiangsu, China) or plasmids sourced from Jikai Company (Shanghai, China), respectively. The siRNA sequences used were as follows: 5'-GCCAGCAUUUACCAGACA UTT-3' and 5'-GCCUCAUACUCGAAACAGUTT-3'. Transfected cells were incubated for 48 h and subsequently employed for ensuing experimental procedures.

Western blotting analysis

Before conducting western blotting analyses, CC cells and xenograft tumor tissues were lysed in RIPA buffer pre-cooled to 4 °C to obtain the total protein. Then we separated the extracted total protein using 10% SDS-PAGE gel electrophoresis, followed by transferring the separated proteins onto nitrocellulose membranes (Millipore, MA, USA) using a constant current of 200 mA. After blocking non-specific proteins with 5% skim milk powder, the membranes were incubated overnight at 4 °C with primary antibodies. Details of the primary antibodies are provided in Supplementary Table 1. Subsequently, the membranes were washed three times with Tris-buffered saline Tween (TBST, T1085, Solarbio, Beijing, China) for 10 min each, followed by incubation with secondary antibodies at room temperature for one hour. After three additional washes, the target proteins were detected using ECL reagent (Yeasen, Shanghai, China).

Immunohistochemistry (IHC) assays

The immunohistochemical staining assays and assessment methods were conducted following established procedures, as detailed in our previous publication [36]. In this study, samples with a score index (SI) less than 6 were categorized as having low RNF6 expression, while those exceeding this threshold were considered to have high RNF6 expression.

Cellular RNA extraction and qRT-PCR analysis

After different treatments, total RNA from CC cells was extracted using TRIzol reagent (9108, Takara Biochemicals, Dalian, China) following the manufacturer's instructions. The reverse transcription of isolated RNA into complementary DNA was performed using reverse transcriptase, oligo(dT) and random primers. The reverse transcription kit was purchased from Takara Biochemicals (RR037A, Takara Biochemicals, Dalian, China). The PCR reaction mixture containing cDNA templates, gene-specific primers, and fluorescent probes (SYBR Green Mix, RR820A, Takara Biochemicals, Dalian, China) was prepared. Real-time quantitative PCR analysis was conducted using the Bio-Rad CFX Connect system (Bio-Rad, Hercules, CA, USA), following the manufacturer's guidelines. The primer sequences used are detailed in Table 2, with GAPDH serving as an internal control. The $2^{-\Delta\Delta Ct}$ method was employed to determine the relative mRNA expression levels of target genes.

Cell counting Kit-8 (CCK-8) and colony formation assays

The CCK-8 assay and colony formation assays were employed to assess cell growth. For the CCK-8 assay, transfected cells (10^3/well) were cultured in 96-well plates and treated with 10 μL of CCK-8 reagent (Beyotime, Shanghai, China) daily for 5 days. After a 2-hour incubation, cell viability was measured at 450 nm using a microplate reader (SpectraMax M5e, CA, USA) to generate growth curves.

In the colony formation assays, equal numbers of transfected CC cells (10^3/well) were seeded into 6-well plates and cultured until visible colonies formed (clusters consisting of more than 50 cells), typically after approximately 2 weeks. The cells were then fixed with 4% paraformaldehyde (PFA) and stained with 1% crystal violet for 20 min at room temperature. ImageJ software facilitated colony counting. Each biological experiment was replicated at least thrice.

Wound healing and Transwell assays

Transfected CC cells were seeded into 6-well plates and cultured until absolutely confluent. A straight line was

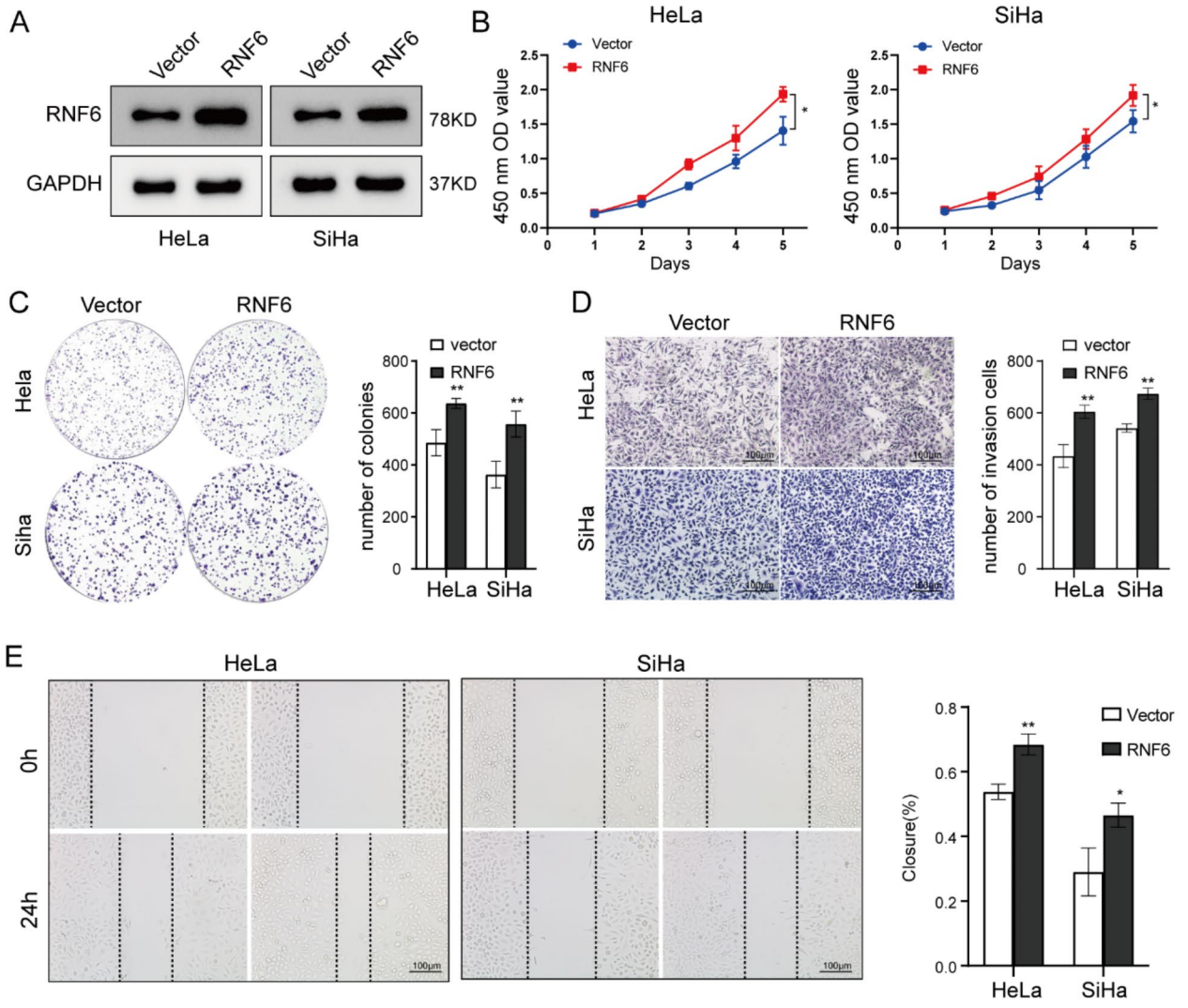

Fig. 2 Elevated levels of RNF6 triggers the aggressive characteristics of CC cells. (**A**) The effectiveness of RNF6 plasmid transfection was evaluated via Western blot analysis in HeLa and SiHa cells. (**B**) Cell viability was evaluated using CCK-8 experiments. (**C-E**) The impact of RNF6 on colony formation, invasion, and migration abilities of CC cells was examined through colony formation experiments, transwell invasion assays, and wound healing assays in cells transfected with Flag-RNF6 or vector. *$p < 0.05$, **$p < 0.01$

drawn on the cell layer using a sterile 10 μL pipette tip to simulate wound formation. Subsequently, careful washing with PBS buffer was performed to ensure cleanliness of the wound area. Cell culture was conducted using serum-free medium, and images were regularly captured during the culture process to evaluate dynamic changes in wound healing, including quantitative analysis of cell migration and healing speed.

A 24-well Transwell plate was taken out, and a diluted mixture of Matrigel was prepared by diluting liquid Matrigel gel and 10 g/L bovine serum albumin (BSA) solution at an 8:1 ratio. The resulting mixture (60 μL) was added to the bottom of the Transwell chamber and incubated at room temperature for 30 min to allow Matrigel gel formation. 50 μL of BSA solution was added to the pores formed on the surface of the Matrigel gel to hydrate the Matrigel gel. Then, transfected CC cells suspension was added to the upper chamber of each well, with an appropriate number of cells, typically 3×10^4 cells. Complete medium was added to the lower chamber to provide sufficient nutrition. Finally, the 24-well Transwell plate was placed in a cell culture incubator at 37 °C and 5% CO_2 for 48 h. After incubation, the plate was removed, and migrated cells were fixed with 4% PFA and stained with 1% crystal violet at room temperature for 20 min. At least five random fields of view were selected for image capture and cell counting. Each experiment was performed in triplicate to validate the repeatability and accuracy of the results.

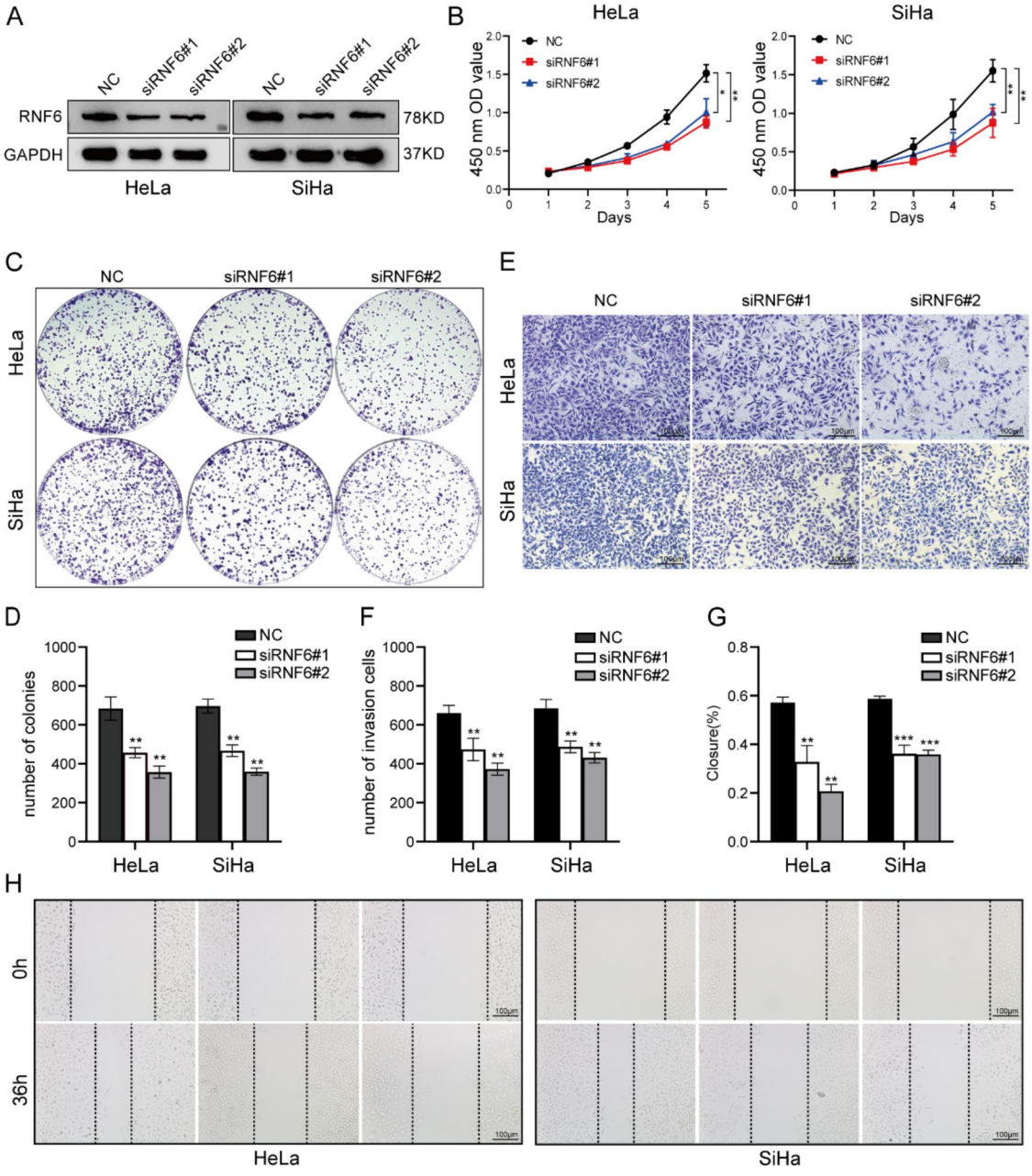

Fig. 3 Silencing RNF6 inhibits the aggressive characteristics of CC cells. (**A**) HeLa and SiHa cells were transfected with RNF6 siRNAs, and western blotting was employed to validate the efficiency of transfection. (**B**) Cell growth upon RNF6 downregulation was assessed using CCK-8 assays. (**C-H**) The impact of RNF6 silencing on cell colony formation, invasion, and migration in CC cells was examined through colony formation assays, transwell invasion assays, and wound healing assays, respectively, in cells transfected with RNF6 siRNAs or scramble shRNA. *$p < 0.05$, **$p < 0.01$

Transcriptome sequencing

We initiated this assay by transfecting RNF6 plasmids into HeLa cells to investigate its role in CC progression. RNA extraction was performed using commercial kits, followed by reverse transcription to convert RNA into cDNA. Barcodes and adapters were incorporated for sample identification and preparation for sequencing. Library amplification was achieved through PCR, with quality control procedures ensuring unbiased conditions. Illumina sequencing was carried out, and raw data underwent quality control, including the removal of low-quality reads. Cleaned reads were aligned to a reference genome, and statistical methods were applied to identify genes with significant expression changes. Functional enrichment and pathway analyses were conducted on differentially expressed genes to shed light on RNF6's specific contribution to CC progression.

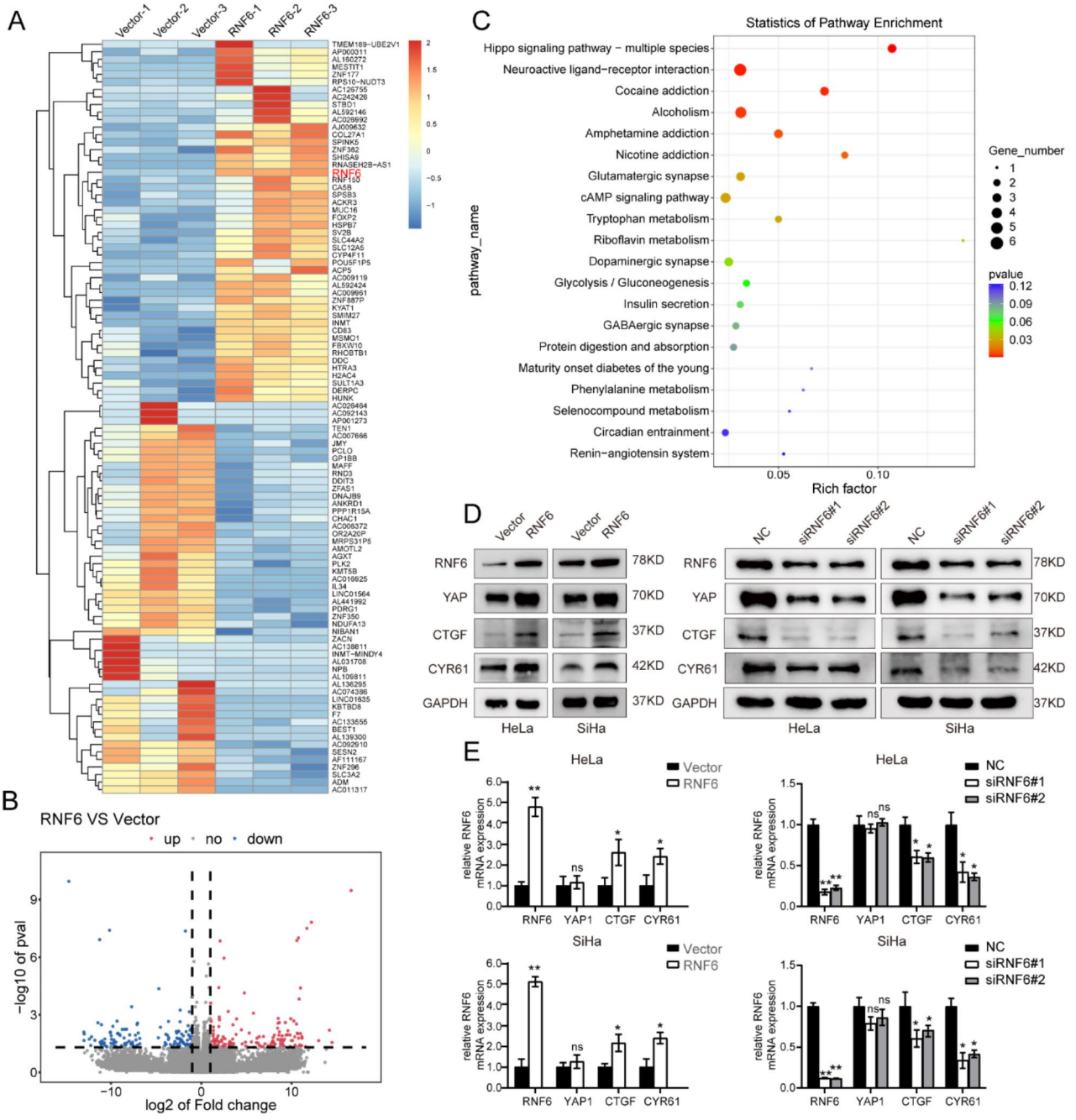

Fig. 4 RNF6 exerts regulatory effects on the YAP signaling pathway. Transfection of the RNF6 overexpression plasmid was conducted in HeLa cells, followed by transcriptome sequencing. (**A**) A heatmap illustrating the overall expression pattern of select differentially expressed genes. (**B**) Expression profile of all genes, with 137 genes upregulated (in red) and 131 genes downregulated (in blue) depicted in a volcano plot. (**C**) KEGG enrichment analysis for differentially expressed genes presented in bubble plots. (**D**, **E**) The protein and mRNA expression of YAP1, and its downstream target genes CYR61 and CTGF detected by Western blot and qRT–PCR in CC cells following modulation of RNF6 expression. *$p < 0.05$, **$p < 0.01$

Animal experiments

The animal experiments began by obtaining female BALB/c nude mice aged 5–6 weeks from Ziyuan Biotech Company (Hangzhou, China). These mice were then randomly split into two groups. The mice were subcutaneously injected in the armpit with 1×10^6 HeLa cells infected with either RNF6 shRNA or scramble shRNA. Over the course of the experiment, tumor growth was closely monitored and measured every three days. Tumor volume was calculated using the formula: Tumor Volume=1/2 × (length × width^2). After 28 days, the mice were euthanized, and their xenograft tumors were

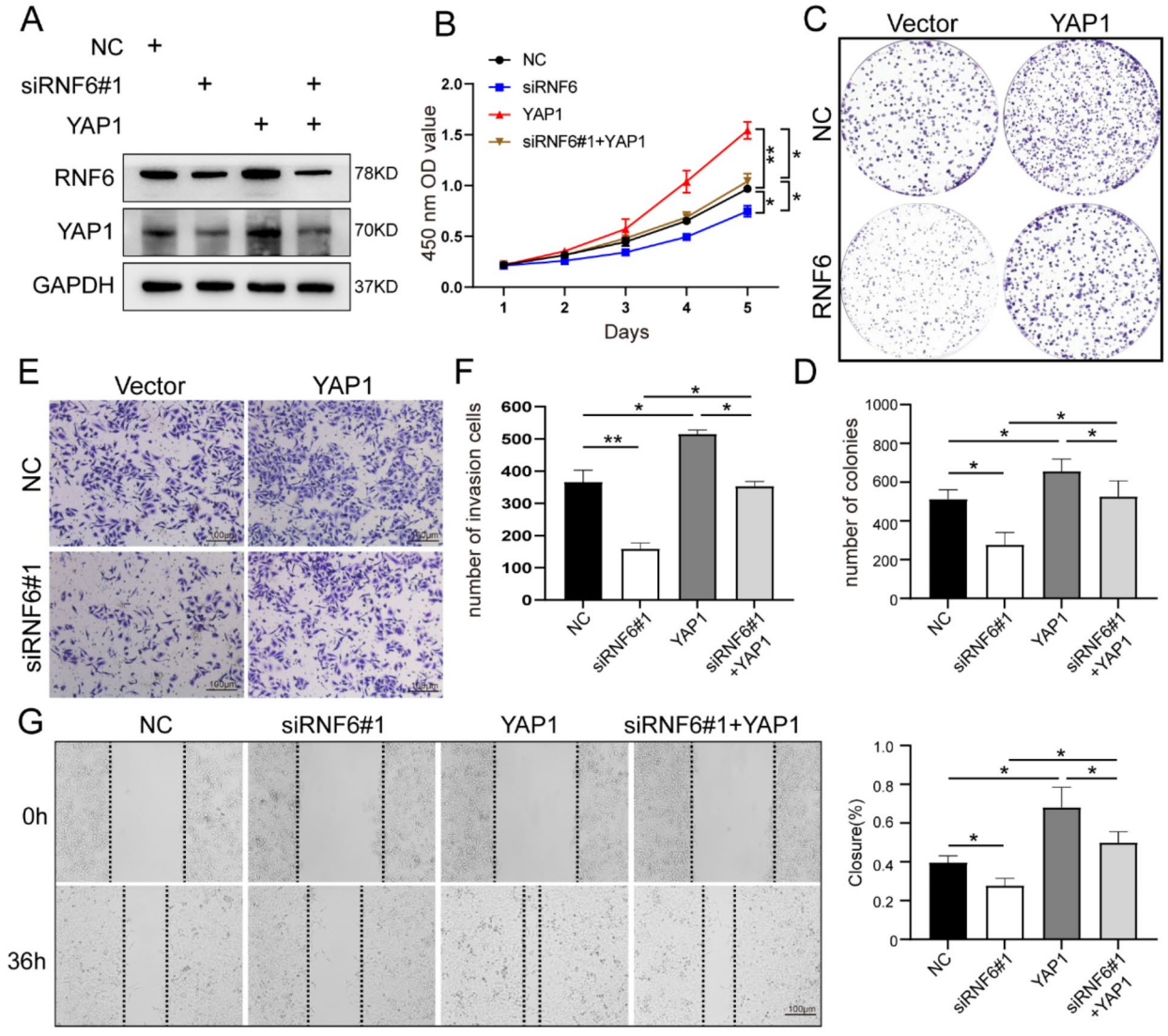

Fig. 5 Ectopic expression of YAP1 reverses the functional phenotypes induced by RNF6 deficiency in CC. (**A**) Western blotting analysis detected the protein expression of RNF6 and YAP1 in RNF6-silenced HeLa cells co-transfected with or without the YAP1 overexpression plasmid. (**B-D**) CCK-8 assays and colony formation assays were conducted using RNF6-silenced HeLa cells co-transfected with or without the YAP1 overexpression plasmid. (**E-G**) Transwell invasion and wound healing assays were utilized to assess the migratory and invasive capacities of RNF6-silenced HeLa cells co-transfected with or without the YAP1 overexpression plasmid. *$p < 0.05$, **$p < 0.01$

removed, weighed, and photographed. Additionally, protein extraction was conducted from the tumor tissues for further analysis via western blotting to explore underlying molecular mechanisms.

Statistical analysis

The statistical analysis was performed utilizing SPSS 27.0 software (Chicago, IL, USA). Group mean differences were assessed using either Student's two-tailed t-test or one-way analysis of variance (ANOVA), as appropriate, and the chi-square test assessed clinicopathological feature discrepancies. Survival curves were constructed employing the Kaplan-Meier method and subsequently assessed via the log-rank test. A significance threshold of $P<0.05$ was set for all analysis. Each experiment was conducted independently on at least three occasions to ensure reliability, and the data were expressed as mean ± standard error of the mean (SEM).

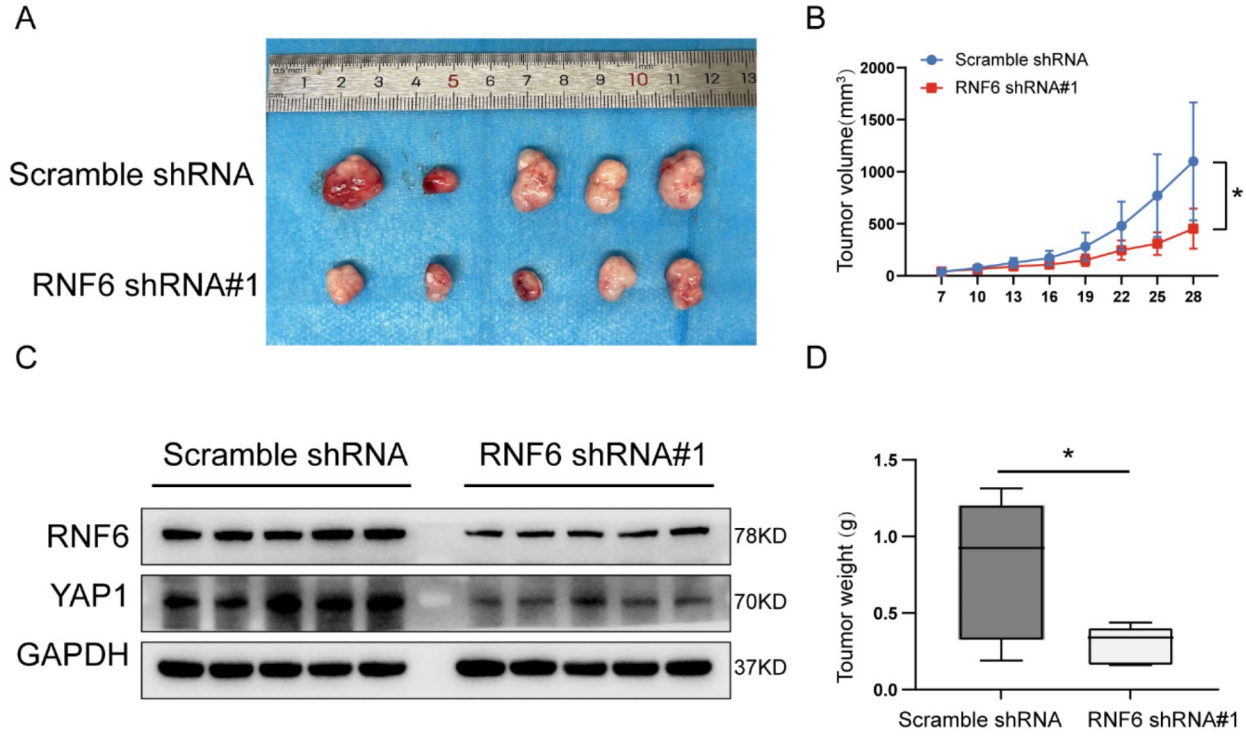

Fig. 6 The depletion of RNF6 attenuated the proliferation of CC cells in vivo. (**A**, **D**) Xenograft tumor images were captured and documented (A), followed by weighing (D) upon completion of the in vivo experiments. (**B**) Growth curves of xenograft tumors originating from HeLa cells transfected with either scramble shRNA or RNF6 shRNA#1 were plotted. (**C**) Evaluation of the RNF6 and YAP1 protein in xenograft tumors by Western blotting. The data are summarized as the mean ± SEM. *$P < 0.05$ by two-tailed t test

Table 2 Primer sequences used in qRT-PCR assays

Gene	Primer sequences
RNF6	Forward: 5′-AAGACCTGGAGAGATGGGCA-3′
	Reverse: 5′-AGGTTTCTTCACTGCCACCA-3′
YAP	Forward: 5′-TCGTTTTGCCATGAACCAGA-3′
	Reverse: 5′-GGCTGCTTCACTGGAGCACT-3′
CYR61	Forward: 5′-CAGGACTGTGAAGATGCGGT-3′
	Reverse: 5′-GCCTGTAGAAGGGAAACGCT-3′
CTGF	Forward: 5′-CCTGGTCCAGACCACAGAGT-3′
	Reverse: 5′-TGGAGATTTTGGGAGTACGG-3′
GAPDH	Forward: 5′-CACCCACTCCTCCACCTTTG-3′
	Reverse: 5′-CCACCACCCTGTTGCTGTAG-3′

Supplementary Information

The online version contains supplementary material available at https://doi.org/10.1186/s13008-024-00136-8.

Supplementary Material 1

Supplementary Material 2

Supplementary Material 3

Supplementary Material 4

Supplementary Material 5

Supplementary Material 6

Acknowledgements
The authors express their gratitude to the Human Genetic Resources Center and Medical Innovation Center of the First Affiliated Hospital of Nanchang University for their invaluable support.

Author contributions
L.L. and L.Z. conceptualized and designed the experiments. Y.L., J.Z., and W.L. executed the experiments, performed data analysis, and contributed to manuscript drafting. Y.L., Z.Z., and L.Z. provided technical assistance and offered critical feedback. Y.L. provided funding for the research. All authors participated in manuscript revision and approved the final version for submission.

Funding
This study was financially supported by the Natural Science Foundation of Jiangxi Province (grant number: 20202BABL216061).

Data availability
No datasets were generated or analysed during the current study.

Declarations

Ethics statement
Our study was approved by Ethics Review Board of the First Affiliated Hospital of the Nanchang University and Jiangxi Maternal and Child Health Hospital.

Competing interests
The authors declare no competing interests.

Conflict of interest
The authors have no relevant financial or non-financial interests to disclose.

Author details
[1]Department of Oncology, Jiangxi Maternal and Child Health Hospital, 318 Bayi Road, 330006 Nanchang, Jiangxi Province, P.R. China
[2]Department of Oncology, the First Affiliated Hospital of Nanchang University, 1519 Dongyue Avenue, 330006 Nanchang, Jiangxi Province, P.R. China
[3]Department of Jiangxi Key Laboratory for Individualized Cancer Therapy, 17 Yongwai Street, 330006 Nanchang, Jiangxi, China

Received: 25 April 2024 / Accepted: 7 November 2024
Published online: 17 November 2024

References

1. Sung H, Ferlay J, Siegel RL, Laversanne M, Soerjomataram I, Jemal A, Bray F. Global Cancer statistics 2020: GLOBOCAN estimates of incidence and Mortality Worldwide for 36 cancers in 185 countries. Cancer J Clin. 2021;71:209–49.
2. Bray F, Ferlay J, Soerjomataram I, Siegel RL, Torre LA, Jemal A. Global cancer statistics 2018: GLOBOCAN estimates of incidence and mortality worldwide for 36 cancers in 185 countries. Cancer J Clin. 2018;68:394–424.
3. Siegel RL, Miller KD, Fuchs HE, Jemal A. Cancer statistics, 2022. CA: a Cancer. J Clin. 2022;72(1):7–33.
4. Sawaya GF, Huchko MJ. Cervical Cancer screening. Med Clin N Am. 2017;101:743–53.
5. McClung NM, Lewis RM, Gargano JW, Querec T, Unger ER, Markowitz LE. Declines in Vaccine-Type human papillomavirus prevalence in females across Racial/Ethnic groups: data from a National Survey. J Adolesc Health. 2019;65:715–22.
6. Miller KD, Nogueira L, Devasia T, Mariotto AB, Yabroff KR, Jemal A, Kramer J, Siegel RL. Cancer treatment and survivorship statistics, 2022. CA: a Cancer. J Clin. 2022;72:409–36.
7. Dey A, Varelas X, Guan K-L. Targeting the Hippo pathway in cancer, fibrosis, wound healing and regenerative medicine. Nat Rev Drug Discovery. 2020;19:480–94.
8. Meng Z, Moroishi T, Guan K-L. Mechanisms of Hippo pathway regulation. Genes Dev. 2016;30(1):1–17.
9. Huang S, Cao Y, Guo H, Yao Y, Li L, Chen J, Li J, Xiang X, Deng J, Xiong J. Up-regulated acylglycerol kinase (AGK) expression associates with gastric cancer progression through the formation of a novel YAP1-AGK-positive loop. J Cell Mol Med. 2020;24:11133–45.
10. Hong AW, Meng Z, Guan K-L. The Hippo pathway in intestinal regeneration and disease. Nat Reviews Gastroenterol Hepatol. 2016;13:324–37.
11. Ma S, Meng Z, Chen R, Guan K-L. The Hippo Pathway: Biology and Pathophysiology. Annu Rev Biochem. 2019;88:577–604.
12. Wang D, He J, Dong J, Meyer TF, Xu T. The HIPPO pathway in gynecological malignancies. Am J Cancer Res. 2020;10:610–29.
13. Huang Y, Zou Y, Jie Z. RNF6 promotes the migration and invasion of breast cancer by promoting the ubiquitination and degradation of MST1. Experimental Therapeutic Med. 2022;23:118.
14. Cai J, Xiong Q, Jiang X, Zhou S, Liu T. RNF6 facilitates metastasis and radioresistance in hepatocellular carcinoma through ubiquitination of FoxA1. Exp Cell Res. 2019;374:152–61.
15. Jiang Q, Miao J, Wu F, Li F, Zhang J, Jing X, Cai S, Ma X, Wang X, Zhao L, Huang C. RNF6 promotes gastric cancer progression by regulating CCNA1/CREBBP transcription. Cell Cycle (Georgetown Tex). 2023;22:2018–37.
16. Sun Y, Sun H, Qi Y, Pan M, An N, Leng X, Liu Y, Chen Z. Ring finger protein 6 enhances chemo-resistance by transcriptionally activating proliferating cell nuclear antigen expression and attenuating DNA damage in lung adenocarcinoma. Cancer Lett. 2022;534:215609.
17. Lo HS, Hu N, Gere S, Lu N, Su H, Goldstein AM, Taylor PR, Lee MP. Identification of somatic mutations of the RNF6 gene in human esophageal squamous cell carcinoma. Cancer Res. 2002;62:4191–3.
18. Li Q, Wang G, Tao J, Chen W. RNF6 promotes colorectal cancer invasion and migration via the Wnt/β-catenin pathway by inhibiting GSK3β activity. Pathol Res Pract. 2021;225:153545.
19. Liu L, Zhang Y, Wong CC, Zhang J, Dong Y, Li X, Kang W, Chan FKL, Sung JJY, Yu J. RNF6 promotes colorectal Cancer by activating the Wnt/β-Catenin pathway via Ubiquitination of TLE3. Cancer Res. 2018;78:1958–71.
20. Cheng J, Wu K, Yang Q, Zhu Z, Zhao H. RNF6 activates TGF-β1/c-Myb pathway to promote EMT in esophageal squamous cell carcinoma. Front Oncol. 2023;13:1081333.
21. Moya IM, Halder G. Hippo-YAP/TAZ signalling in organ regeneration and regenerative medicine. Nat Rev Mol Cell Biol. 2019;20:211–26.
22. He C, Mao D, Hua G, Lv X, Chen X, Angeletti PC, Dong J, Remmenga SW, Rodabaugh KJ, Zhou J, et al. The Hippo/YAP pathway interacts with EGFR signaling and HPV oncoproteins to regulate cervical cancer progression. EMBO Mol Med. 2015;7:1426–49.
23. Zhao X, Fu J, Hu B, Chen L, Wang J, Fang J, Ge C, Lin H, Pan K, Fu L, et al. Serine metabolism regulates YAP activity through USP7 in Colon cancer. Front Cell Dev Biology. 2021;9:639111.
24. Dong L, Lin F, Wu W, Liu Y, Huang W. Verteporfin inhibits YAP-induced bladder cancer cell growth and invasion via Hippo signaling pathway. Int J Med Sci. 2018;15:645–52.
25. Gao Y, Yang Y, Yuan F, Huang J, Xu W, Mao B, Yuan Z, Bi W. TNFα-YAP/p65-HK2 axis mediates breast cancer cell migration. Oncogenesis. 2017;6:e383.
26. Nguyen CDK, Yi C. YAP/TAZ signaling and resistance to Cancer Therapy. Trends Cancer. 2019;5:283–96.
27. Yap T, Desai J, Dagogo-Jack I, Millward M, Kindler HL, Tolcher AW, Frentzas S, Body AL, Thurston A, Post L et al. P2.19-01 first-in-human phase 1 trial of VT3989, a first-in-class YAP/TEAD inhibitor in patients with Advanced Mesothelioma. J Thorac Oncol 2023, 18.
28. Huang Z, Cai Y, Yang C, Chen Z, Sun H, Xu Y, Chen W, Xu D, Tian W, Wang H. Knockdown of RNF6 inhibits gastric cancer cell growth by suppressing STAT3 signaling. OncoTargets Therapy. 2018;11:6579–87.
29. Jin ZD, Chang L, Zhu LL. RNF6 serves as a diagnostic hallmark of non-alcoholic fatty liver disease with hepatocellular carcinoma: a clinical research. Eur Rev Med Pharmacol Sci. 2020;24:11052–7.
30. Zhu H, Wang C. Potential influences of RNF6 on prognosis and metastasis of Colorectal Cancer: a clinical analysis. OncoTargets Therapy. 2020;13:2031–6.
31. Zhu K, Bai H, Mu M, Xue Y, Duan Z. Knockdown of RNF6 inhibits HeLa cervical cancer cell growth via suppression of MAPK/ERK signaling. FEBS Open Bio. 2021;11:2041–9.
32. La Starza R, Wlodarska I, Aventin A, Falzetti D, Crescenzi B, Van den Martelli MF, Mecucci C. Molecular delineation of 13q deletion boundaries in 20 patients with myeloid malignancies. Blood. 1998;91:231–7.
33. Cai C, Tang Y-D, Zhai J, Zheng C. The RING finger protein family in health and disease. Signal Transduct Target Therapy. 2022;7:300.
34. Tang M, Zeng X, Luo J, Quan F-F, Chen C-Y, Li Y-K, Liu J, Zhang Q-F. Gene commander in the trash heap: transcriptional regulation and ubiquitination modification mediated by RNF6 in carcinogenesis. Exp Cell Res. 2021;401:112396.
35. Xu H, Wong CC, Li W, Zhou Y, Li Y, Wang L, Liu L, Yu J. RING-finger protein 6 promotes colorectal tumorigenesis by transcriptionally activating SF3B2. Oncogene. 2021;40:6513–26.
36. Zhou L, Guo H, Liao Q, Zou J, Le Y, Fang Z, Xiong J, Huang S, Deng J, Xiang X. miR-3133 inhibits gastrointestinal cancer progression through activation of Hippo and p53 signalling pathways via multi-targets. J Cell Mol Med. 2023;27:3090–106.

Publisher's note